

# Modulation of the antitumor activity of metronomic cyclophosphamide by the angiogenesis inhibitor axitinib

Jie Ma and David J. Waxman

Division of Cell and Molecular Biology, Department of Biology, Boston University, Boston, Massachusetts

## Abstract

The promising but still limited efficacy of angiogenesis inhibitors as monotherapies for cancer treatment indicates a need to integrate these agents into existing therapeutic regimens. Presently, we investigate the antitumor activity of the small-molecule angiogenesis inhibitor axitinib (AG-013736) and its potential for combination with metronomic cyclophosphamide. Axitinib significantly inhibited angiogenesis in rat 9L tumors grown s.c. in *scid* mice but only moderately delayed tumor growth. Combination of axitinib with metronomic cyclophosphamide fully blocked 9L tumor growth on initiation of drug treatment. In contrast, metronomic cyclophosphamide alone required multiple treatment cycles to halt tumor growth. However, in contrast to the substantial tumor regression that is ultimately induced by metronomic cyclophosphamide, the axitinib/cyclophosphamide combination was tumor growth static. Axitinib did not inhibit hepatic activation of cyclophosphamide or export of its activated metabolite, 4-hydroxy-cyclophosphamide (4-OH-CPA), to extrahepatic tissues; rather, axitinib selectively decreased 9L tumor uptake of 4-OH-CPA by 30% to 40%. The reduced tumor penetration of 4-OH-CPA was associated with a decrease in cyclophosphamide-induced tumor cell apoptosis and a block in the induction of the endogenous angiogenesis inhibitor thrombospondin-1 in tumor-associated host cells, which may contribute to the absence of tumor regression with the axitinib/cyclophosphamide combination. Finally, axitinib transiently increased 9L tumor cell apoptosis, indicating that its effects are not limited to the endothelial cell population. These findings highlight the multiple effects that may characterize antiangiogenic agent/metronomic chemotherapy combinations and suggest that careful optimization of drug scheduling and dosages will be required to maximize antitumor responses. [Mol Cancer Ther 2008;7(1):79–89]

Received 8/21/07; revised 11/9/07; accepted 12/4/07.

Grant support: NIH grant CA49248 (D.J. Waxman).

The costs of publication of this article were defrayed in part by the payment of page charges. This article must therefore be hereby marked *advertisement* in accordance with 18 U.S.C. Section 1734 solely to indicate this fact.

Requests for reprints: David J. Waxman, Division of Cell and Molecular Biology, Department of Biology, Boston University, 5 Cummington Street, Boston, MA 02215. Fax: 617-353-7404. E-mail: djw@bu.edu

Copyright © 2008 American Association for Cancer Research.

doi:10.1158/1535-7163.MCT-07-0584

## Introduction

Since the approval of bevacizumab for use in combination with 5-fluorouracil-based chemotherapy for metastatic colorectal cancer in 2004, several antiangiogenic drugs have been approved for cancer treatment and others are progressing through preclinical and clinical development (1, 2). Many of these new agents primarily target the vascular endothelial growth factor signaling pathway, inducing rapid vasoconstriction by decreasing the relaxation of pericytes and smooth muscle cells followed by slower responses, including the inhibition of new blood vessel formation and pruning of immature vessels (3). Antiangiogenic drugs are typically cytostatic rather than cytoreductive and often show moderate efficacy when used as monotherapies, highlighting the importance of integrating these new treatment options with traditional cancer therapies (4, 5). In some but not all cases, antiangiogenic drug treatments normalize the tumor vasculature, thereby facilitating the delivery of chemotherapeutic drugs and oxygen into the tumor and improving therapeutic responses (6). However, the optimal dose needs to be determined carefully for each antiangiogenic drug and likely for each combination therapy.

Metronomic chemotherapy involves the administration of a chemotherapeutic drug at a reduced dose compared with traditional treatment regimens but at regular, more frequent intervals without extended rest periods (7, 8). In contrast to traditional maximum tolerated dose therapy, metronomic chemotherapy not only is cytotoxic against tumor cells but also exerts an antiangiogenic effect toward tumor-associated endothelial cells. The antiendothelial activity can in part be explained by the high intrinsic sensitivity of proliferating endothelial cells to chemotherapeutic drugs and by the induction of the endogenous angiogenesis inhibitor thrombospondin-1 (TSP-1; refs. 7, 9, 10). The most extensively studied metronomic chemotherapy uses the oxazaphosphorine alkylating agent cyclophosphamide, which can be administered on an every 6-day schedule or continuously (11, 12). The antitumor effect of metronomic cyclophosphamide can be further improved by using gene therapy vectors to effect intratumoral expression of a cyclophosphamide-activating cytochrome *P450* enzyme as shown in preclinical studies (13, 14).

Axitinib (AG-013736) is a potent small-molecule inhibitor of the vascular endothelial growth factor receptor (15). The antitumor activity of axitinib is accompanied by significant antiangiogenic effects (16–19). However, axitinib typically exerts tumor cytostatic activity, which results in an encouraging but still limited efficacy in the monotherapy setting. The combination of axitinib with other treatment regimens, such as cytotoxic and antiangiogenic metronomic chemotherapy, is an important objective. Furthermore, it is

important to evaluate the effect of the antiangiogenic actions of axitinib on the delivery of chemotherapeutic drugs included in the combination therapies. To address these issues, we presently investigate the effects of axitinib in combination with metronomic cyclophosphamide in preclinical studies using 9L gliosarcoma, a highly vascularized tumor model.

## Materials and Methods

### Chemicals

Axitinib (15, 16) was supplied by Pfizer Global Research and Development. Cyclophosphamide, NADPH, semicarbazide hydrochloride, crystal violet, and mouse monoclonal antibody to  $\alpha$ -smooth muscle actin (A-5228) were purchased from Sigma-Aldrich. 4-Hydroperoxycyclophosphamide (4-HC) was obtained from Dr. Ulf Niemeyer (Baxter Oncology GmbH). Methanol [high-performance liquid chromatography (HPLC) grade] was purchased from J.T. Baker. Paraformaldehyde solution (16%; methanol-free) was purchased from Electron Microscopy Sciences. Polyethylene glycol 400 and 1% alcoholic eosin Y were purchased from Fisher Scientific. Mouse monoclonal anti-proliferating cell nuclear antigen antibody (2586) was purchased from Cell Signaling Technology. Rat monoclonal anti-CD31 antibody (557355) was purchased from BD Bioscience. Normal rabbit serum, normal horse serum, avidin/biotin blocking kit, biotinylated rabbit anti-rat antibody (BA-4000), biotinylated horse anti-mouse antibody (BA-2000), VECTASTAIN Elite ABC Kit, peroxidase substrate VIP, VectaMount, and Gill's hematoxylin were purchased from Vector Laboratories. DeadEnd Colorimetric terminal deoxynucleotidyl transferase-mediated dUTP nick end labeling (TUNEL) kit and RNase-free DNase were purchased from Promega. Hypoxyprobe-1 kit, including pimonidazole, was purchased from Chemicon. DMEM, fetal bovine serum, and TRIzol were purchased from Invitrogen. EGM-2 BulletKit endothelial cell culture medium was purchased from Cambrex Bio Science. High-capacity cDNA Reverse Transcription Kit, RNase inhibitor, and SYBR Green PCR Master Mix were purchased from Applied Biosystems.

### Cell Lines

Rat gliosarcoma cell lines 9L and 9L/2B11 were those described previously (14). Cells were grown in DMEM with 10% fetal bovine serum at 37°C in a humidified, 5% CO<sub>2</sub> atmosphere. The 9L cell model was chosen based on its high vascularity (20, 21), and earlier studies where the therapeutic responses to metronomic cyclophosphamide treatment have been extensively tested (13, 14). Human umbilical vein endothelial cells were purchased from Cambrex Bio Science and were grown in EGM-2 BulletKit endothelial cell culture medium.

### Tumor Growth Delay Experiments

Immunodeficient male Fox Chase ICR *scid* mice were purchased from Taconic and housed in the Boston University Laboratory of Animal Care Facility in accordance with approved protocols and federal guidelines. Autoclaved cages containing food and water were changed

once a week. Mouse body weight was monitored every 3 to 4 days. On the day of tumor cell inoculation, 9L tumor cells at 70% to 80% confluence were trypsinized and resuspended in fetal bovine serum-free DMEM. Cells ( $4 \times 10^6$ ) in a volume of 0.2 mL were injected s.c. into each flank of a 5-week-old mouse (body weight, 20-22 g; 2 tumors per mouse). Tumor sizes were measured every 3 to 4 days using digital calipers (VWR International) and volumes were calculated as  $(3.14/6) \times (L \times W)^{3/2}$ . Mice were randomized to different groups on the day of initial drug treatment when the average tumor volume reached  $\sim 500 \text{ mm}^3$  (10-24 tumors per group, as specified; average body weight, 28-30 g). Axitinib dissolved in 3 parts of polyethylene glycol 400 and 7 parts of acidified water (pH 2-3) was administered to the tumor-bearing mice daily by i.p. injection at 25 mg/kg body weight. Initial experiments showed that similar antitumor responses were induced by axitinib (25 mg/kg i.p.) given either every 12 h or once a day (Supplementary Fig. S1).<sup>1</sup> Therefore, a once-daily axitinib treatment schedule was used for all subsequent studies. Freshly prepared cyclophosphamide dissolved in PBS (140 mmol/L NaCl, 10 mmol/L Na<sub>2</sub>HPO<sub>4</sub>, 2.7 mmol/L KCl, 1.8 mmol/L KH<sub>2</sub>PO<sub>4</sub>) was filtered through a 0.2- $\mu\text{m}$  acrodisc syringe filter and administered by i.p. injection at 140 mg cyclophosphamide/kg body weight every 6 days (i.e., a metronomic treatment schedule; refs. 11, 13). In the combination treatment studies, on those days when cyclophosphamide and axitinib were both administered, cyclophosphamide was injected 4 h before axitinib to minimize the potential for drug interactions. This time interval was chosen based on the findings that 4 h after i.p. injection of cyclophosphamide the concentration of its activated metabolite, 4-hydroxy-cyclophosphamide (4-OH-CPA), has already decreased to the detected limit in blood, liver, and tumor (see Fig. 4B; Supplementary Table S1).<sup>1</sup>

### Immunohistochemical Staining, Tumor Microvessel Density, and Proliferation Index

Pimonidazole hydrochloride (60 mg/kg body weight) was injected i.p. to *scid* mice bearing 9L tumors 60 min before the mice were killed by cervical dislocation. Tumor tissues were excised and snap frozen in dry ice-cold 2-methylbutane and stored at  $-80^\circ\text{C}$  as described (21). Briefly, 1% paraformaldehyde-fixed tumor cryosections (6  $\mu\text{m}$ ) were detergent permeabilized then treated with 3% H<sub>2</sub>O<sub>2</sub> for 5 min to block endogenous peroxidase. Sections were blocked with 2% normal serum then incubated with primary antibody (1 h at 37°C then two PBS washes) and then secondary antibody (1 h at room temperature then three PBS washes). The sections were incubated with ABC complex and then stained with the peroxidase substrate VIP. Following hematoxylin counterstaining, the slides were dehydrated and sealed with VectaMount. The final concentration (or dilution) of each primary antibody was

<sup>1</sup> Supplementary material for this article is available at Molecular Cancer Therapeutics Online (<http://mct.aacrjournals.org/>).

as follows: anti-CD31 (0.3  $\mu\text{g}/\text{mL}$ ), Hypoxyprobe-1 (1:50), anti-proliferating cell nuclear antigen (1:1,000), and anti- $\alpha$ -smooth muscle actin (5  $\mu\text{g}/\text{mL}$ ). Biotinylated anti-rat or anti-mouse secondary antibodies were diluted to 7.5  $\mu\text{g}/\text{mL}$ . Immunostained tumor sections were examined using an Olympus BX51 bright-field light microscope. The number of CD31<sup>+</sup> blood vessels was counted at  $\times 400$  magnification for a maximal number of non-overlapping fields covering each section. The number of blood vessels with pericyte coverage (that is, vessels positive for  $\alpha$ -smooth muscle actin immunostaining) was measured in the same way at  $\times 200$  magnification. The number of proliferating cell nuclear antigen-positive cells per field at  $\times 200$  magnification was counted as an index of tumor cell proliferation. Microvessel density, pericyte-covered vessel density, and proliferation index data are presented as counts per field (mean  $\pm$  SE) typically based on 20 to 60 fields for each of four individual tumors.

#### TUNEL Assay and Apoptotic Index

Axitinib-treated tumors were collected 24 h after the last axitinib injection, except for the 12-h time point, where tumors were collected 12 h after a single i.p. injection of axitinib. Tumors were collected 48 h after the last cyclophosphamide injection from mice treated with cyclophosphamide or with the axitinib/cyclophosphamide combination. TUNEL assay was done according to the manufacturer's protocol with modifications (21). TUNEL-positive cells were counted at  $\times 200$  magnification for the maximal number of fields covering each section. The average number of apoptotic cells per field (that is, apoptotic index) was calculated and expressed as mean  $\pm$  SE for four individual tumors.

#### Effect of Axitinib on Tissue Uptake of 4-OH-CPA

The effect of axitinib on cyclophosphamide metabolism to 4-OH-CPA and on 4-OH-CPA uptake by target tissues was determined as follows. A single i.p. injection of cyclophosphamide (140 mg/kg body weight) was administered to untreated mice 24 h after the last axitinib treatment, except in the case of the 12-h time point, where cyclophosphamide was given 12 h after axitinib. Mice were killed 15 min after cyclophosphamide injection, corresponding to the  $t_{\text{max}}$  of 4-OH-CPA in plasma, liver, and tumor (22). Blood samples were collected by cardiac puncture. Liver, tumor, kidney, and heart tissues were homogenized on ice in 0.1 mol/L KPi buffer (pH 7.4) containing 5 mmol/L semicarbazide hydrochloride to stabilize the 4-OH-CPA. After 30-min centrifugation at  $130 \times g$  at 4°C, 500  $\mu\text{L}$  supernatant (or 50  $\mu\text{L}$  plasma diluted in 450  $\mu\text{L}$  KPi buffer) was deproteinized by the sequential addition of 250  $\mu\text{L}$  of 5.5% zinc sulfate and 250  $\mu\text{L}$  saturated BaOH. Acrolein formed during chemical decomposition of 4-OH-CPA was derivatized to 7-hydroxyquinoline and analyzed by HPLC (23, 24). A standard curve for 4-OH-CPA was generated using 4-HC (0-40  $\mu\text{mol}/\text{L}$ ) dissolved in KPi buffer and processed in parallel. 4-HC is a chemically activated derivative of cyclophosphamide that spontaneously decomposes to 4-OH-CPA in

aqueous solution. Integrated peak areas determined by Millennium software (Waters) were converted to units of nanomole of 4-OH-CPA produced per gram of tissue. Tissue recovery of 4-OH-CPA was determined to be  $60 \pm 3\%$  with a sensitivity of 1  $\mu\text{mol}/\text{L}$  under these conditions (24). Data were expressed as mean  $\pm$  SE for six tumors (three mice) per data point.

#### Pharmacokinetic Analysis of 4-OH-CPA Metabolism and Distribution

Mice bearing 9L tumors were given a single i.p. injection of cyclophosphamide (140 mg/kg) without any pretreatment or were treated with axitinib (25 mg/kg i.p. s.i.d. for 4 days) followed by cyclophosphamide injection 24 h later. Tissues were collected 6, 15, 30, 60, 120, or 240 min after cyclophosphamide injection, and levels of 4-OH-CPA were determined by HPLC as described above. WinNonlin software (Standard Edition, version 1.5; noncompartmental and extravascular input setting) was used to calculate area under the curve,  $C_{\text{max}}$ ,  $t_{\text{max}}$ , and  $t_{1/2}$  for 4-OH-CPA in plasma, tumor, liver, kidney, and heart. Data were expressed as mean  $\pm$  SE based on three individual mice or six individual tumors per time point.

#### Cell Growth Inhibition Assay

Axitinib stock solution (10 mmol/L in DMSO) was stored at  $-20^\circ\text{C}$ . 9L or human umbilical vein endothelial cells were seeded in triplicate wells of a 24-well plate and grown overnight followed by addition of axitinib at concentrations ranging from 1 nmol/L to 10  $\mu\text{mol}/\text{L}$ . The cells were cultured for 4 days in the presence of axitinib, washed twice with PBS on ice, and then quantified by crystal violet staining at 595 nm (25). The staining intensity of drug-treated samples was calculated as a percentage of untreated controls. The effect of axitinib treatment on tumor cell sensitivity to 4-OH-CPA was determined using 4-HC. 9L tumor cells were treated with one of the following schedules: (a) DMSO control for 2 days followed by 4-HC treatment for 4 days, (b) DMSO control for 2 days followed by 4-HC plus axitinib for 4 days, or (c) axitinib for 2 days followed by 4-HC plus axitinib for 4 days. For both axitinib and 4-HC treatments, drug exposure was limited to 4 h daily to mimic the pharmacokinetic profiles of 4-OH-CPA and axitinib exposure *in vivo*, following which the cells were incubated in fresh drug-free culture medium. Twenty four hours after the last treatment, the remaining cells were washed twice with PBS, stained, and quantified by crystal violet staining.  $\text{IC}_{50}$  values were calculated using sigmoidal concentration-response analysis with a variable slope as implemented in Prism version 4.0 software (GraphPad).

#### Real-time PCR

TSP-1 RNA was quantified by quantitative, real-time PCR using SYBR Green I chemistry. Tumor samples were collected 24 h after last drug treatment, snap frozen in liquid nitrogen, and stored at  $-80^\circ\text{C}$ . Total RNA isolation from frozen tumor samples (0.1-0.4 g) using TRIzol reagent, reverse transcription, and PCR were carried out as described (21).  $C_T$  values determined for each mRNA were normalized to the 18S rRNA content.

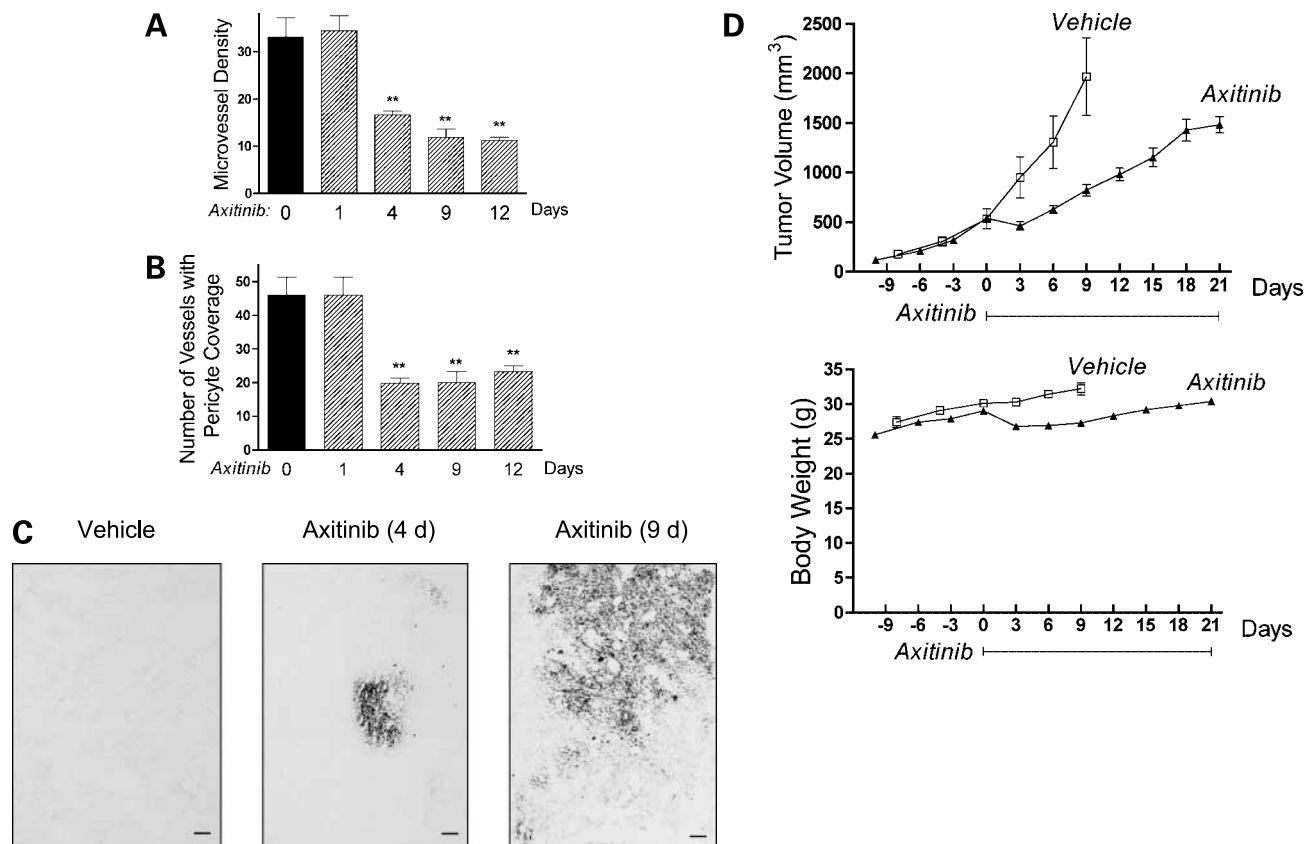


**Figure 1.** Antiangiogenic activity and tumor growth delay of axitinib monotherapy in rat 9L gliosarcoma. 9L tumors grown s.c. in *scid* mice were treated with axitinib for up to 21 d at 25 mg/kg i.p. s.i.d. **A**, number of tumor blood vessels per CD31-immunostained 9L tumor section counted at  $\times 400$  magnification. Axitinib significantly reduced microvessel density after 4 to 12 d of treatment. **B**, effect of axitinib treatment on the number of 9L tumor blood vessels with pericyte coverage, identified as  $\alpha$ -smooth muscle actin-positive blood vessels at  $\times 200$  magnification. X axis, days of axitinib treatment (4 tumors per group). \*\*,  $P < 0.01$ , compared with day 0 controls (**A** and **B**). **C**, immunostaining for hypoxia-specific dye pimonidazole revealed an increase in tumor hypoxia after 4 and 9 d of axitinib treatment. Bar, 100  $\mu$ m. **D**, axitinib treatment initiated on day 0 delayed 9L tumor growth (*top*; 10 tumors per group) with minimal effect on the rate of mouse body weight gain (*bottom*). Solid line along X axis, period of daily axitinib treatment.

### Statistical Analysis

Results were expressed as mean  $\pm$  SE and are based on the indicated number of tumors or tissue samples per group. Statistical significance of differences was assessed by two-tailed Student's *t* test using Prism software with statistical significance indicated by \*  $P < 0.05$ , \*\*  $P < 0.01$ , and \*\*\*  $P < 0.001$ . All time points were compared with day 0 unless specified otherwise.

## Results

### Axitinib Induces Antiangiogenic Responses and Delays 9L Tumor Growth

When used as a monotherapy, daily axitinib treatment induced a strong antiangiogenic response in 9L tumors within 4 days as shown by a significant decrease in tumor vascular density (Fig. 1A) and by a decline in the number of blood vessels with pericyte coverage (Fig. 1B). Axitinib also increased tumor hypoxia (Fig. 1C). 9L tumor growth was initially inhibited by axitinib treatment (days 0-3; Fig. 1D, *top*) at which time there was a small but transient decrease in

mouse body weight (Fig. 1D, *bottom*). Tumor growth subsequently resumed, albeit at a rate slower than in the vehicle-treated control tumors. Axitinib thus has a limited antitumor effect in the 9L gliosarcoma model. This antitumor activity was not enhanced by increasing the frequency of axitinib treatment to twice daily (Supplementary Fig. S1).<sup>1</sup>

### Axitinib/Metronomic Cyclophosphamide Combination Therapy Is 9L Tumor Growth Static

Coadministration of axitinib with metronomic cyclophosphamide blocked 9L tumor growth soon after the initiation of drug treatment (Fig. 2A). By contrast, metronomic cyclophosphamide given as a monotherapy required two to three treatment cycles to achieve tumor growth inhibition. However, whereas metronomic cyclophosphamide regressed 9L tumors, the combination of axitinib with metronomic cyclophosphamide induced tumor growth stasis but not tumor regression. This tumor stasis effect was sustained for a prolonged period, with limited regression ultimately observed in mice where daily axitinib treatment was continued through day 24 and metronomic cyclophosphamide treatment continued until day

48 (Fig. 2A). Similar responses were observed with 9L tumors that express P450 2B11 (9L/2B11 tumors; Fig. 2B), which activate cyclophosphamide to 4-OH-CPA intratumorally (22) and display increased and more complete tumor regression following metronomic cyclophosphamide

treatment (14). Moreover, whereas metronomic cyclophosphamide substantially decreased 9L tumor cell density after five treatment cycles, as revealed by H&E staining, this effect was not observed with the axitinib/cyclophosphamide combination (Fig. 2C). A small but tolerable body

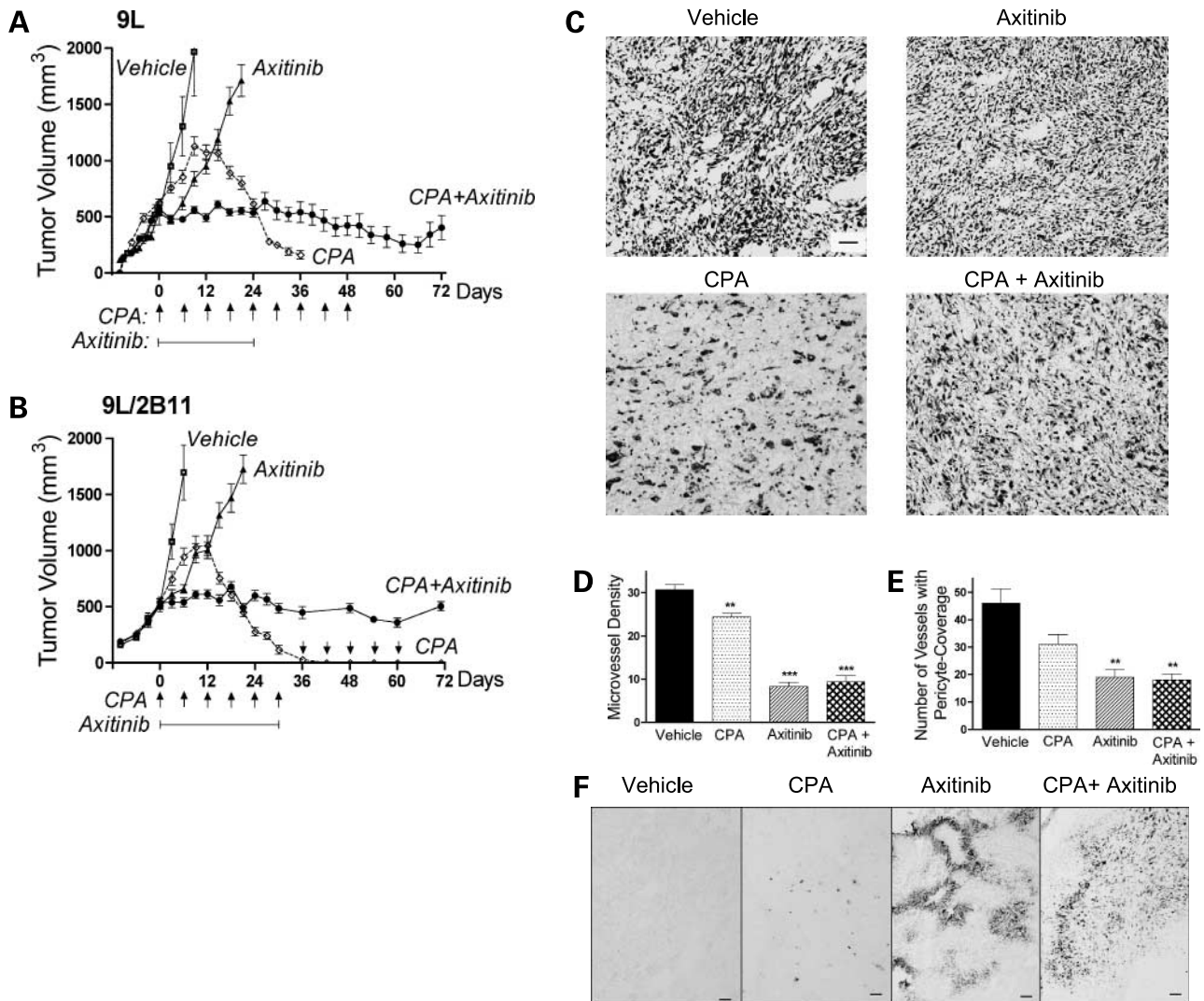


**Figure 2.** Axitinib/metronomic cyclophosphamide combination blocks 9L tumor growth but does not induce tumor regression. **A** and **B**, 9L tumors (**A**) or 9L/2B11 tumors (**B**), which can activate cyclophosphamide intratumorally, were implanted s.c. in *scid* mice, grown to an average volume of 500 mm<sup>3</sup>, and then treated with the axitinib/metronomic cyclophosphamide combination (see Materials and Methods). Cyclophosphamide-induced tumor regression (most complete for 9L/2B11 tumors) was absent in the combination treatment group, which displayed sustained tumor growth stasis, continuing even after termination of drug treatment. *Arrows along the X axis*, days of cyclophosphamide treatment (140 mg/kg i.p. every 6 d); *solid line below the arrows*, period of axitinib treatment (25 mg/kg i.p. s.i.d.). On the days when both drugs were coadministered, cyclophosphamide was given 4 h before axitinib to minimize drug-drug interactions. For 9L tumors (**A**), there were 20 to 24 tumors per group through day 24, after which 6 tumors were left for longer-term monitoring, whereas the other tumor samples were collected for analysis. In case of 9L/2B11 tumors (**B**), there were 10 tumors per group through day 30, after which both drug treatments were terminated for the cyclophosphamide plus axitinib combination group and 3 mice (or 6 tumors) were removed for tissue analysis; the remaining 4 tumors were monitored until day 72. For the cyclophosphamide-treated 9L/2B11 tumors, cyclophosphamide administration on an every 6-day schedule was continued for the 4 remaining tumors from days 30 to 60 (*arrows above X axis*) and tumor measurements continued until day 72. **C**, 9L tumor cryosections prepared from mice receiving the indicated treatments were stained with H&E. Similar tumor cell morphologies and cell densities were observed in tumors from mice treated with vehicle, axitinib (25 mg/kg i.p. s.i.d. for 21 d), or the combination therapy (26 d). In contrast, metronomic cyclophosphamide (140 mg/kg i.p. every 6 d for 26 d) induced changes in both cell morphology and density. Bar, 50  $\mu$ m. **D**, microvessel density of CD31-immunostained 9L tumor cryosections measured at  $\times 400$  magnification. **E**, number of blood vessels with  $\alpha$ -smooth muscle actin-positive pericyte coverage counted at  $\times 200$  magnification. **F**, antiangiogenic activity of the axitinib/cyclophosphamide combination was manifested by increased tumor hypoxia as detected by pimonidazole staining. Bar, 100  $\mu$ m. Drug treatments for **D** to **F** were the same as described in **C**. **D** and **E**, four tumors per group. \*\*,  $P < 0.01$ ; \*\*\*,  $P < 0.001$ , compared with vehicle controls.

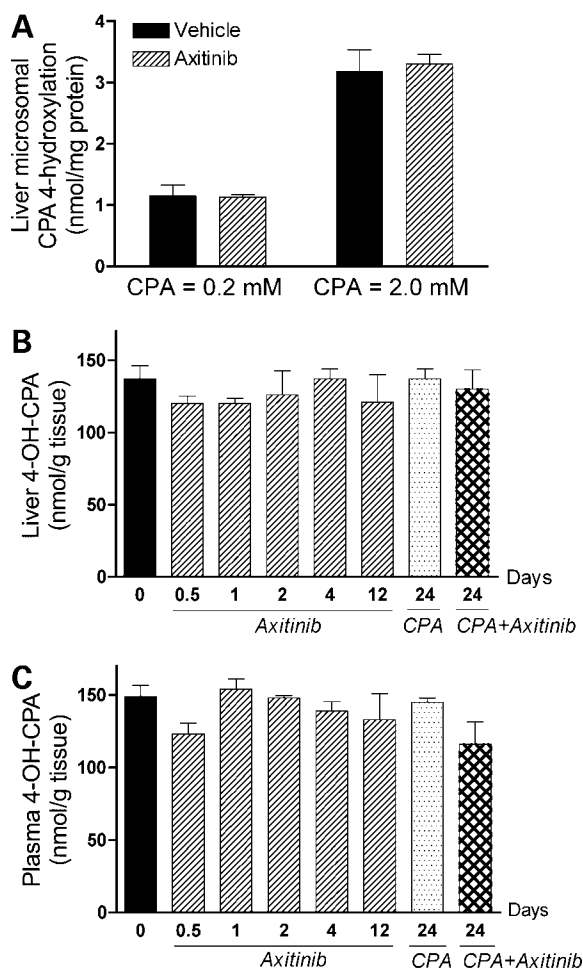


**Figure 3.** Effect of axitinib treatment on hepatic activation of cyclophosphamide and export of its active metabolite, 4-OH-CPA. **A**, mice bearing 9L tumors were treated with vehicle or axitinib (25 mg/kg i.p. s.i.d.) for 4 d. Twenty-four hours after the last drug injection, liver microsomes were isolated (21) and 4-OH-CPA activity was assayed by HPLC (23) following *in vitro* incubation with 0.2 or 2 mmol/L cyclophosphamide. Mean  $\pm$  SE based on three livers per group. The levels of 4-OH-CPA in liver (**B**) and plasma (**C**) were measured by HPLC 15 min after injection of a single test dose of cyclophosphamide (140 mg/kg, i.p.). The 15-min time point corresponds to the  $t_{max}$  (4-OH-CPA; see Fig. 4B). None of the values shown is significantly different than the day 0 (untreated) controls (The 3 mice per group;  $P > 0.05$  for all treatments compared with controls). Numbers along the X axis, period of drug treatment as described in Fig. 2.

weight loss was associated with the combination therapy (Supplementary Fig. S2).<sup>1</sup> Axitinib monotherapy and the axitinib/metronomic cyclophosphamide combination both showed enhanced antiangiogenic responses (Fig. 2D and E) associated with increased tumor hypoxia (Fig. 2F) when compared with metronomic cyclophosphamide treatment alone.

#### Axitinib Does Not Affect Hepatic Cyclophosphamide Activation or 4-OH-CPA Export to Plasma

Next, we investigated why 9L tumor regression induced by metronomic cyclophosphamide was blocked by the axitinib/cyclophosphamide combination, which fully

retained the strong antiangiogenic effects associated with axitinib alone. First, we determined that axitinib does not alter hepatic cytochrome P450-catalyzed cyclophosphamide activation, as shown by analysis of liver microsomal cyclophosphamide 4-hydroxylase activity, determined at two cyclophosphamide concentrations (Fig. 3A). Moreover, HPLC analysis of 4-OH-CPA concentrations in liver and plasma 15 min after a single i.p. injection of cyclophosphamide indicated no major effect of prior treatment with axitinib, cyclophosphamide, or the combination on the export of 4-OH-CPA from liver to systemic circulation (Fig. 3B and C; Supplementary Fig. S3)<sup>1</sup>.

#### Axitinib Significantly Reduces the Exposure of 9L Tumors to 4-OH-CPA

The effect of the axitinib-induced decrease in 9L tumor vascular density on tumor uptake of 4-OH-CPA was determined by assaying intratumoral 4-OH-CPA concentrations 15 min after i.p. injection of cyclophosphamide. Twelve hours after the first axitinib treatment, tumor uptake of 4-OH-CPA was decreased by  $\sim 40\%$ , with no further change apparent after 12 daily axitinib treatments (Fig. 4A). Moreover, whereas 9L tumor 4-OH-CPA levels decreased by only 16% after four metronomic cyclophosphamide treatment cycles (that is, 24 days), the axitinib/

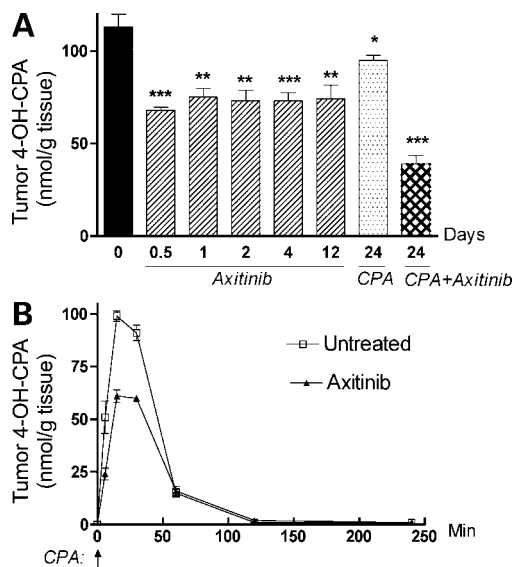


**Figure 4.** Effect of axitinib or axitinib/cyclophosphamide combination on 9L tumor 4-OH-CPA exposure. **A**, levels of 4-OH-CPA in 9L tumors treated with axitinib (25 mg/kg i.p. s.i.d.), metronomic cyclophosphamide (140 mg/kg i.p. every 6 d), or the combination for the indicated periods of time were measured 15 min after injection of a test dose of cyclophosphamide as described in Fig. 3. Intratumoral 4-OH-CPA uptake was decreased  $\sim 40\%$  within 12 h after the first axitinib injection and remained at that level through 12 daily axitinib treatments. Four cycles of the combination treatment decreased 4-OH-CPA uptake by 9L tumors by  $>60\%$ . \*,  $P < 0.05$ ; \*\*,  $P < 0.01$ ; \*\*\*,  $P < 0.001$ , compared with day 0 controls, with six tumors per group. **B**, levels of 4-OH-CPA in untreated or axitinib-pretreated (25 mg/kg i.p. s.i.d. for 4 d) 9L tumors were measured 6 to 240 min after a single test dose of cyclophosphamide (vertical arrow at 0 min, single i.p. injection at 140 mg/kg). Area under the curve for tumor 4-OH-CPA exposure decreased from 4,545 to 3,251 nmol/g min after 4 d of axitinib treatment (see Supplementary Table S1), with six tumors per time point.

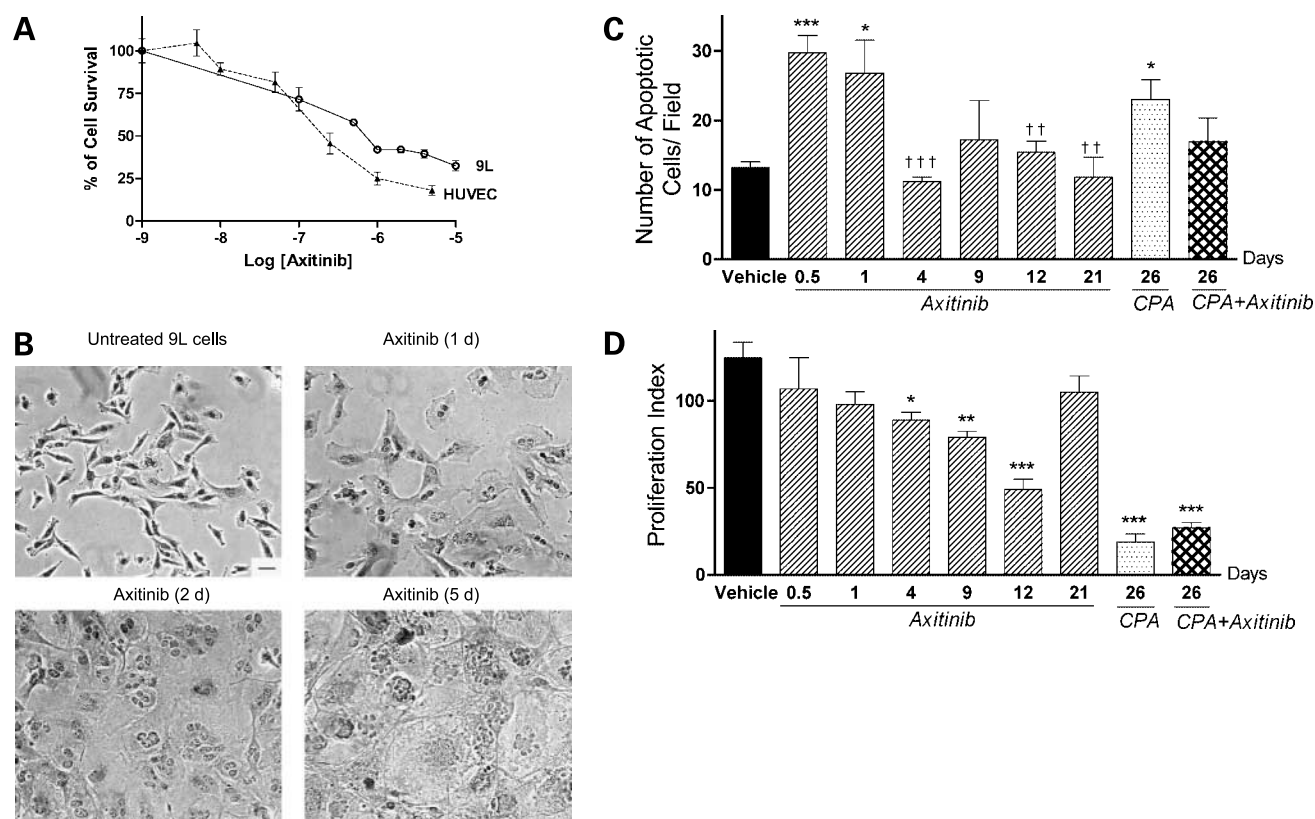


**Figure 5.** Direct effects of axitinib on 9L tumor cells. **A**, cultured 9L tumor cells and human umbilical vein endothelial cells were treated with axitinib at the indicated concentrations for 4 d and the effect on final cell number, indicative of relative growth rate, was determined by crystal violet staining (3 replicates per data point). **B**, morphology of H&E-stained 9L cells treated with axitinib (500 nmol/L) for up to 5 d in culture. Bar, 50  $\mu$ m. The effect of the indicated *in vivo* drug treatments on tumor cell apoptosis (**C**) and proliferation (**D**) was analyzed by TUNEL assay and proliferating cell nuclear antigen immunostaining, respectively. The number of staining-positive cells was counted at  $\times 200$  magnification. *Numbers along the X axis*, period of drug treatment, as described in Figs. 2 and 3. \*,  $P < 0.05$ ; \*\*,  $P < 0.01$ ; \*\*\*,  $P < 0.001$ , compared with day 0 controls. †,  $P < 0.05$ ; ††,  $P < 0.01$ ; †††,  $P < 0.001$ , compared with the response at 12 h (day 0.5), with four tumors per group.

metronomic cyclophosphamide combination reduced intratumoral 4-OH-CPA levels by  $>60\%$  (Fig. 4A). In contrast, the axitinib/cyclophosphamide combination did not affect 4-OH-CPA uptake by kidney and heart (Supplementary Fig. S3).<sup>1</sup> A more detailed pharmacokinetic analysis verified that 4 days of axitinib pretreatment decreased net tumor exposure to 4-OH-CPA as judged by a 30% decrease in area under the curve and a 36% decrease in  $C_{\max}$  ( $P < 0.0001$ ; Fig. 4B; Supplementary Table S1).<sup>1</sup> The area under the curve (4-OH-CPA) was unchanged in plasma, liver, heart, and kidney (Supplementary Table S1),<sup>1</sup> showing that axitinib selectively decreases tumor exposure to 4-OH-CPA, which likely contributes to the absence of tumor regression with the combination treatment.

#### Axitinib Has Limited Direct Effect on 9L Tumor Cells

In addition to an antiangiogenic mechanism, the possibility of direct targeting of tumor cells by axitinib was investigated. In cell culture, axitinib inhibited 9L cell growth at concentrations moderately higher than those required for inhibition of human umbilical vein endothelial cells (Fig. 5A). Moreover, axitinib induced significant morphological changes in the cultured 9L cells as indicated

by the appearance of multiple nuclei and an enlarged cell size (Fig. 5B). Careful examination of H&E-stained tumor sections did not reveal such morphological changes in axitinib-treated 9L tumors (cf. Fig. 2C), indicating that the axitinib treatment regimen has limited effect on tumor cell morphology *in vivo*. However, TUNEL labeling revealed an early increase in apoptotic cells in axitinib-treated 9L tumors (Fig. 5C), which may contribute to the initial growth inhibition that accompanied axitinib treatment. These TUNEL-positive cells are primarily composed of 9L tumor cells, insofar as the overall number of apoptotic endothelial cells was very low and not significantly increased by axitinib treatment (Supplementary Fig. S4).<sup>1</sup> The apoptotic effect of axitinib on 9L tumor cells was no longer apparent after four daily axitinib treatments. Forty-eight hours after the fifth cyclophosphamide treatment cycle (that is, on day 26), the number of 9L tumor apoptotic cells was increased in the cyclophosphamide alone group but not with the axitinib/cyclophosphamide combination (Fig. 5C). Axitinib had little or no effect on the intrinsic chemosensitivity of cultured 9L cells to activated cyclophosphamide, added in the form of 4-HC (Supplementary

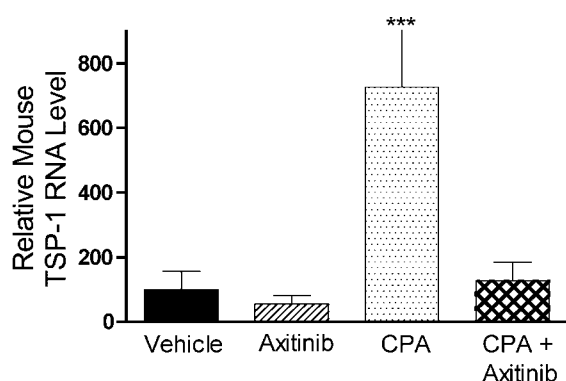


**Figure 6.** Expression of mouse TSP-1 RNA after multiple drug treatments. The level of host (mouse) TSP-1 RNA in 9L tumor was measured by real-time PCR following treatment with axitinib (25 mg/kg i.p. s.i.d. for 21 d), metronomic cyclophosphamide (140 mg/kg i.p. every 6 d for 26 d), or the combination (26 d). Metronomic cyclophosphamide induced a 7-fold increase in mouse TSP-1 expression, which was absent in axitinib-treated or the combination therapy-treated tumors. Data are expressed as mean  $\pm$  SE relative RNA levels for four to eight individual tumors per group.

Table S2)<sup>1</sup>. Thus, reduced tumor penetration of 4-OH-CPA rather than a decrease in intrinsic chemosensitivity accounts for the decrease in cyclophosphamide-induced apoptosis in the axitinib/cyclophosphamide-treated tumors. Analysis of the 9L tumor cell proliferation profile by proliferating cell nuclear antigen staining revealed a steady decrease of proliferating cells in the first 12 days of axitinib treatment, with a recovery to the untreated level by day 21 (Fig. 5D). An even lower 9L tumor cell proliferation index was seen after treatment with metronomic cyclophosphamide or the axitinib/cyclophosphamide combination (Fig. 5D, *last two columns*), and this may contribute to the tumor regression and growth stasis effects, respectively, induced by these treatments.

#### Metronomic Cyclophosphamide-Induced Mouse TSP-1 Expression Is Blocked in the Combination Therapy

Metronomic cyclophosphamide treatment of 9L tumors induces the expression of TSP-1, an endogenous angiogenesis inhibitor (21). This increase in host (mouse) TSP-1 was confirmed in the present study (Fig. 6). Moreover, although mouse TSP-1 expression was not affected by axitinib, the axitinib/cyclophosphamide combination completely blocked the increase in TSP-1 induced by metronomic cyclophosphamide. Given the essential role of TSP-1 for the antitumor action of metronomic cyclophosphamide (26), this block in TSP-1 induction may contribute to the inability of the combination therapy to regress 9L tumors. The expression of 9L tumor (that is, rat) TSP-1 was not affected by any of the treatments, and limited changes (<2-fold) in total (mouse + rat) TSP-1 RNA were observed in the axitinib-treated and combination therapy-treated 9L tumors (data not shown).

#### Discussion

Axitinib is a potent small-molecule receptor tyrosine kinase inhibitor that induces significant antiangiogenic responses,

including rapid loss of tumor vascular potency with a decrease in tumor blood volume followed by a gradual decrease in microvessel density and >90% loss of endothelial fenestration of the tumor vasculature (16, 17). These strong antiangiogenic responses contribute to the antitumor activity of axitinib but also raise questions as to how they will affect the pharmacokinetics and pharmacodynamics of more traditional cancer chemotherapeutics in a combination therapy setting. In the present study, we used rat 9L gliosarcoma, a highly vascularized tumor model (20, 21), to study the combination of daily axitinib administration with cyclophosphamide given on an every 6-day repeating, metronomic treatment schedule (11, 13). We found that the combination therapy induced sustained tumor growth stasis on initiation of drug treatment. However, the strong antiangiogenic effect of this drug combination substantially decreased intratumoral levels of 4-OH-CPA, the liver cytochrome P450-activated metabolite of cyclophosphamide, decreasing the efficacy of the combination therapy. In addition, metronomic cyclophosphamide induction of the host (mouse) antiangiogenic factor TSP-1 was blocked by axitinib, which may help explain why axitinib converts the strong tumor regression response affected by metronomic cyclophosphamide alone to a tumor growth stasis response. Thus, axitinib can modulate the antitumor activity of cyclophosphamide, and potentially other chemotherapeutic drugs, in multiple and complex ways. Further studies will be required to ascertain whether optimization of the dosing and timing of antiangiogenic agents, such as axitinib, can enhance their therapeutic effectiveness while circumventing the undesirable drug interactions described here.

Previous efforts to optimize combinations of angiogenesis inhibitors with traditional radiation or chemotherapy have met with varying degrees of success (27–31). Mechanisms proposed to explain how tumor-starving drugs may improve the efficacy of coadministered chemotherapeutic agents include the normalization of tumor vasculature, inhibition of repair of chemotherapy-induced damage, and stimulation of an antitumor immune response (4, 6, 32). However, the therapeutic benefits of combining angiogenesis inhibitors with radiation or chemotherapy are not universal (5). In the present study, the combination of axitinib with metronomic cyclophosphamide fully blocked 9L tumor growth on initiation of treatment, a response, which in the absence of axitinib, requires several cycles of metronomic cyclophosphamide treatment. An unanticipated finding, however, was that axitinib blocked metronomic cyclophosphamide-induced tumor regression despite the strong antiangiogenic activity of the axitinib/cyclophosphamide combination. Investigation of the effect of axitinib on cyclophosphamide metabolism revealed no effect on the activation of cyclophosphamide to 4-OH-CPA in the liver or on the export of 4-OH-CPA to plasma or its uptake by heart and kidney. This latter finding is consistent with the report that axitinib does not affect vascular densities in heart and kidney (33). In contrast, intratumoral 4-OH-CPA levels were decreased by ~40% within 12 h of a single



axitinib injection, reducing the exposure of 9L tumors to 4-OH-CPA significantly as shown by a 30% decrease in area under the curve and a 36% decline in  $C_{max}$ . This decrease in tumor cell exposure to 4-OH-CPA in the combination therapy setting is supported by the reduced apoptotic index in 9L tumors on day 26 of the axitinib/cyclophosphamide treatment and by the greater similarities in tumor cell morphology and tumor cell density of the combination therapy samples to vehicle-treated tumors than to tumors treated with metronomic cyclophosphamide alone. Of note, the decreases in tumor uptake of 4-OH-CPA preceded changes in tumor vascular density and were not accompanied by increased apoptosis of tumor-associated endothelial cells. They are thus likely to result from functional changes to the tumor vasculature, such as a decrease in vascular potency and/or a reduction in tumor blood volume, which have been observed in other tumor models within 1 day of axitinib treatment (16, 17, 34).

9L tumor vascular density was progressively reduced over a 12-day period of axitinib treatment, whereas the capacity of 9L tumors to take up 4-OH-CPA was decreased ~40% within 12 h, with no further changes seen over the next 12 days. This suggests that the longer-term exposure to axitinib increases the efficiency of blood flow and 4-OH-CPA transport in the remaining tumor blood vessels. Increases in transport efficiency per surviving vessel have been reported for the delivery of IgG protein and 50-nm microspheres to axitinib-treated tumors (35). Axitinib also induces multiple morphological changes, including an increase in the uniformity of tumor blood vessel diameter, a decrease in blood vessel tortuosity and in the number of leaky vessels, and a closer association between pericytes and endothelial cells (16). However, to maintain or even improve drug delivery, normalization of tumor vasculature by antiangiogenic drug treatment requires that there be a sufficient number of surviving blood vessels that retain potency. In the current study, any normalization effect of axitinib on 9L tumor vasculature is counterbalanced by a more dramatic decrease in vascular density and/or a drop in potency. The net result is a decrease in drug penetration and an increase in tumor hypoxia. After 24 days of the combined axitinib/cyclophosphamide treatment, intratumoral 4-OH-CPA levels were further decreased, which may contribute to the inability of the combination therapy to induce tumor regression.

Several other antiangiogenic agents have a direct effect on the delivery of chemotherapeutic drugs to tumors. For example, TNP-470 reduced intratumoral levels of temozolomide (36), whereas intratumoral levels of 4-OH-CPA were increased when cyclophosphamide was administered during the transient blood vessel normalization window induced by thalidomide treatment (37). Blocking of vascular endothelial growth factor receptor signaling by specific antibody induces a transient increase in drug uptake in several tumor models (38–40), but the ability of small-molecule receptor tyrosine kinase inhibitors to enhance drug uptake is largely unknown. The concurrent inhibition of vascular endothelial growth factor, platelet-

derived growth factor, and potentially other tyrosine kinase receptor signaling pathways by such agents may enhance antiangiogenic responses but may also have a substantial negative effect on chemotherapeutic drug delivery as shown here in the case of axitinib. Conceivably, improved delivery of anticancer drugs, and improved chemosensitization, may be achieved by lowering the dose of the antiangiogenic agent. For many antiangiogenic drugs, treatment dosages are typically optimized in a monotherapy setting and then employed in subsequent combination therapy regimens. However, the optimal dose for an antiangiogenic drug used as a chemosensitizing agent in combination chemotherapy may be different from the dose that maximally inhibits tumor angiogenesis. Improvements may be realized through careful dose-response studies in the combination setting as well as from an appropriate sequencing of angiogenesis inhibitors with cytotoxic drugs as proposed by Pietras and Hanahan (27).

As a monotherapy, axitinib delayed the growth of 9L tumors in association with its substantial antiangiogenic effects, which included a decrease in vascular density and an increase in tumor hypoxia. The transient growth inhibitory effect of axitinib was accompanied by a transient increase in apoptosis, seen within 12 to 24 h of a single axitinib treatment, suggesting that tumor cells or non-endothelial stromal cells may be direct targets of axitinib. The mechanisms for this cytotoxic effect and for the transient nature of this response are not known. In cell culture, axitinib inhibited 9L tumor cell growth and induced substantial morphological changes (Fig. 5B). However, whereas axitinib initially increased nonendothelial cell apoptosis *in vivo*, the level of apoptosis returned to pretreatment levels in subsequent cycles of drug treatment, and the morphology of axitinib-treated 9L tumor cells was similar to that seen in untreated tumors. A progressive decline in cell proliferation induced by axitinib treatment, which could be a secondary response to angiogenesis inhibition, was also reversed by day 21 and was accompanied by continued tumor growth. These observations suggest that the axitinib treatment regimen employed here did not have a sustained direct effect on 9L tumor cells, which could indicate the development of resistance to axitinib, for example, by inhibition of tumor blood perfusion, which might limit the delivery of axitinib itself.

The antiangiogenic and antitumor effects of metronomic cyclophosphamide require the endogenous angiogenesis inhibitor TSP-1 (10, 26). In the 9L tumor model, TSP-1 RNA is induced by metronomic cyclophosphamide in host (mouse) cells (21), where TSP-1 protein was primarily localized to perivascular cells, although the number of TSP-1-positive blood vessels was low (Supplementary Fig. S5).<sup>1</sup> Interestingly, although basal TSP-1 levels were not affected by axitinib alone, the induction of host TSP-1 by metronomic cyclophosphamide was blocked by axitinib. Given the requirement of TSP-1 for the antitumor effect of metronomic cyclophosphamide noted above, the block in TSP-1 induction may be another important factor in limiting the effect of axitinib/cyclophosphamide to tumor

growth stasis despite the strong antiangiogenic activity of the drug combination. Further studies will be required to test this hypothesis and to ascertain the mechanism whereby axitinib blocks the induction of TSP-1 in tumor-associated host cells. One possible mechanism is that this is a secondary effect of reduction of 4-OH-CPA levels in the tumors. Further studies with other tumors are also needed to ascertain whether this observation applies to other tumor models as well.

In summary, the angiogenesis inhibitor axitinib is shown to modulate the antitumor activity of metronomic cyclophosphamide in multiple ways. A transient proapoptotic activity of axitinib is associated with a rapid decrease of blood vessel perfusion and may lead to the immediate halt of tumor growth that characterizes the combination therapy. However, the decreased delivery of 4-OH-CPA into the tumor and a block in the induction of tumor-associated host TSP-1 by metronomic cyclophosphamide limit the activity of the combination to tumor growth stasis rather than tumor regression. Thus, the balance between decreasing tumor microvessel density and improving drug uptake by a normalized tumor vasculature needs to be carefully considered as doses and schedules for axitinib and other antiangiogenic drugs are developed for use in a combination chemotherapy setting.

#### Acknowledgments

We thank Pfizer Global Research and Development for providing axitinib, Dr. Dana Hu-Lowe (Pfizer Global Research and Development) for useful discussions, Chong-Sheng Chen for HPLC analysis, and Selen Karaca for assistance with immunohistochemistry.

#### References

- Jain RK, Duda DG, Clark JW, Loeffler JS. Lessons from phase III clinical trials on anti-VEGF therapy for cancer. *Nat Clin Pract Oncol* 2006;3:24–40.
- Ferrara N, Kerbel RS. Angiogenesis as a therapeutic target. *Nature* 2005;438:967–74.
- Ellis LM. Mechanisms of action of bevacizumab as a component of therapy for metastatic colorectal cancer. *Semin Oncol* 2006;33:51–7.
- Kerbel RS. Antiangiogenic therapy: a universal chemosensitization strategy for cancer? *Science* 2006;312:1171–5.
- Nieder C, Wiedenmann N, Andratschke N, Molls M. Current status of angiogenesis inhibitors combined with radiation therapy. *Cancer Treat Rev* 2006;32:348–64.
- Jain RK. Normalization of tumor vasculature: an emerging concept in antiangiogenic therapy. *Science* 2005;307:58–62.
- Kerbel RS, Kamen BA. The anti-angiogenic basis of metronomic chemotherapy. *Nat Rev Cancer* 2004;4:423–36.
- Hanahan D, Bergers G, Bergsland E. Less is more, regularly: metronomic dosing of cytotoxic drugs can target tumor angiogenesis in mice. *J Clin Invest* 2000;105:1045–7.
- Bocci G, Nicolaou KC, Kerbel RS. Protracted low-dose effects on human endothelial cell proliferation and survival *in vitro* reveal a selective angiogenic window for various chemotherapeutic drugs. *Cancer Res* 2002;62:6938–43.
- Bocci G, Francia G, Man S, Lawler J, Kerbel RS. Thrombospondin 1, a mediator of the antiangiogenic effects of low-dose metronomic chemotherapy. *Proc Natl Acad Sci U S A* 2003;100:12917–22.
- Browder T, Butterfield CE, Kraling BM, et al. Antiangiogenic scheduling of chemotherapy improves efficacy against experimental drug-resistant cancer. *Cancer Res* 2000;60:1878–86.
- Man S, Bocci G, Francia G, et al. Antitumor effects in mice of low-dose (metronomic) cyclophosphamide administered continuously through the drinking water. *Cancer Res* 2002;62:2731–5.
- Jounaidi Y, Waxman DJ. Frequent, moderate-dose cyclophosphamide administration improves the efficacy of cytochrome *P*-450/cytochrome *P*-450 reductase-based cancer gene therapy. *Cancer Res* 2001;61:4437–44.
- Jounaidi Y, Chen C-S, Veal GJ, Waxman DJ. Enhanced antitumor activity of *P*450 prodrug-based gene therapy using the low *K*<sub>m</sub> cyclophosphamide 4-hydroxylase *P*450 2B11. *Mol Cancer Ther* 2006;5:541–55.
- Wickman G, Hallin M, Dillon R, et al. Further characterization of the potent VEGF/PDGF receptor tyrosine kinase inhibitor, AG-013736, in preclinical tumor models for its antiangiogenesis and antitumor activity. *Proc Am Assoc Cancer Res*; 2003. p. A3780.
- Inai T, Mancuso M, Hashizume H, et al. Inhibition of vascular endothelial growth factor (VEGF) signaling in cancer causes loss of endothelial fenestrations, regression of tumor vessels, and appearance of basement membrane ghosts. *Am J Pathol* 2004;165:35–52.
- Kim YR, Yudina A, Figueiredo J, et al. Detection of early antiangiogenic effects in human colon adenocarcinoma xenografts: *in vivo* changes of tumor blood volume in response to experimental VEGFR tyrosine kinase inhibitor. *Cancer Res* 2005;65:9253–60.
- Wilmes LJ, Pallavicini MG, Fleming LM, et al. AG-013736, a novel inhibitor of VEGF receptor tyrosine kinases, inhibits breast cancer growth and decreases vascular permeability as detected by dynamic contrast-enhanced magnetic resonance imaging. *Magn Reson Imaging* 2007;25:319–27.
- Rugo HS, Herbst RS, Liu G, et al. Phase I trial of the oral antiangiogenesis agent AG-013736 in patients with advanced solid tumors: pharmacokinetic and clinical results. *J Clin Oncol* 2005;23:5474–83.
- Kirsch M, Strasser J, Allende R, Bello L, Zhang J, Black PM. Angiostatin suppresses malignant glioma growth *in vivo*. *Cancer Res* 1998;58:4654–9.
- Ma J, Waxman DJ. Collaboration between hepatic and intratumoral prodrug activation in a *P*450 prodrug-activation gene therapy model for cancer treatment. *Mol Cancer Ther* 2007;6:2879–90.
- Chen CS, Jounaidi Y, Su T, Waxman DJ. Enhancement of intratumoral cyclophosphamide pharmacokinetics and antitumor activity in a *P*450 2B11-based cancer gene therapy model. *Cancer Gene Ther* 2007;14:935–44.
- Chen CS, Lin JT, Goss KA, He YA, Halpert JR, Waxman DJ. Activation of the anticancer prodrugs cyclophosphamide and ifosfamide: identification of cytochrome *P*450 2B enzymes and site-specific mutants with improved enzyme kinetics. *Mol Pharmacol* 2004;65:1278–85.
- Yu LJ, Drewes P, Gustafsson K, Brain EGC, Hecht JED, Waxman DJ. *In vivo* modulation of alternative pathways of *P*-450-catalyzed cyclophosphamide metabolism: impact on pharmacokinetics and antitumor activity. *J Pharmacol Exp Ther* 1999;288:928–37.
- Schwartz PS, Waxman DJ. Cyclophosphamide induces caspase 9-dependent apoptosis in 9L tumor cells. *Mol Pharmacol* 2001;60:1268–79.
- Hamano Y, Sugimoto H, Soubasakos MA, et al. Thrombospondin-1 associated with tumor microenvironment contributes to low-dose cyclophosphamide-mediated endothelial cell apoptosis and tumor growth suppression. *Cancer Res* 2004;64:1570–4.
- Pietras K, Hanahan D. A multitargeted, metronomic, and maximum-tolerated dose “chemo-switch” regimen is antiangiogenic, producing objective responses and survival benefit in a mouse model of cancer. *J Clin Oncol* 2005;23:939–52.
- Folkens C, Man S, Xu P, Shaked Y, Hicklin DJ, Kerbel RS. Anticancer therapies combining antiangiogenic and tumor cell cytotoxic effects reduce the tumor stem-like cell fraction in glioma xenograft tumors. *Cancer Res* 2007;67:3560–4.
- Huber PE, Bischof M, Jenne J, et al. Trimodal cancer treatment: beneficial effects of combined antiangiogenesis, radiation, and chemotherapy. *Cancer Res* 2005;65:3643–55.
- Hurwitz H, Fehrenbacher L, Novotny W, et al. Bevacizumab plus irinotecan, fluorouracil, and leucovorin for metastatic colorectal cancer. *N Engl J Med* 2004;350:2335–42.
- Klement G, Huang P, Mayer B, et al. Differences in therapeutic indexes of combination metronomic chemotherapy and an anti-VEGFR-2 antibody in multidrug-resistant human breast cancer xenografts. *Clin Cancer Res* 2002;8:221–32.

32. Jinushi M, Dranoff G. Triggering tumor immunity through angiogenesis targeting. *Clin Cancer Res* 2007;13:3762–4.
33. Kamba T, Tam BY, Hashizume H, et al. VEGF-dependent plasticity of fenestrated capillaries in the normal adult microvasculature. *Am J Physiol Heart Circ Physiol* 2006;290:H560–76.
34. Reichardt W, Hu-Lowe D, Torres D, Weissleder R, Bogdanov A, Jr. Imaging of VEGF receptor kinase inhibitor-induced antiangiogenic effects in drug-resistant human adenocarcinoma model. *Neoplasia* 2005;7:847–53.
35. Nakahara T, Norberg SM, Shalinsky DR, Hu-Lowe DD, McDonald DM. Effect of inhibition of vascular endothelial growth factor signaling on distribution of extravasated antibodies in tumors. *Cancer Res* 2006;66:1434–45.
36. Ma J, Pulfer S, Li S, Chu J, Reed K, Gallo JM. Pharmacodynamic-mediated reduction of temozolomide tumor concentrations by the angiogenesis inhibitor TNP-470. *Cancer Res* 2001;61:5491–8.
37. Segers J, Fazio VD, Ansiaux R, et al. Potentiation of cyclophosphamide chemotherapy using the anti-angiogenic drug thalidomide: importance of optimal scheduling to exploit the “normalization” window of the tumor vasculature. *Cancer Lett* 2006;244:129–35.
38. Tong RT, Boucher Y, Kozin SV, Winkler F, Hicklin DJ, Jain RK. Vascular normalization by vascular endothelial growth factor receptor 2 blockade induces a pressure gradient across the vasculature and improves drug penetration in tumors. *Cancer Res* 2004;64:3731–6.
39. Dickson PV, Hamner JB, Sims TL, et al. Bevacizumab-induced transient remodeling of the vasculature in neuroblastoma xenografts results in improved delivery and efficacy of systemically administered chemotherapy. *Clin Cancer Res* 2007;13:3942–50.
40. Wildiers H, Guetens G, De Boeck G, et al. Effect of antivascular endothelial growth factor treatment on the intratumoral uptake of CPT-11. *Br J Cancer* 2003;88:1979–86.